Relativistic description of exclusive semileptonic decays of heavy mesons

R. N. Faustov, V. O. Galkin, and A. Yu. Mishurov
Russian Academy of Sciences, Scientific Council for Cybernetics, Vavilov Street 40, Moscow, 117333, Russia
(Received 5 June 1995)

Using the quasipotential approach, we study exclusive semileptonic decays of heavy mesons taking into account relativistic effects. Because of a more complete relativistic description of the s quark, more precise expressions for semileptonic form factors are obtained. Various differential distributions in exclusive semileptonic decays of heavy mesons are calculated. It is argued that a consistent account of relativistic effects and a heavy quark effective theory motivated choice of the parameters of the quark-antiquark potential allow one to get a reliable value for the ratio $A_2(0)/A_1(0)$ in the $D \to K^* l\nu_l$ decay as well as the ratio $\Gamma(D \to K^* l\nu_l)/\Gamma(D \to K l\nu_l)$. All calculated branching ratios are in accord with available experimental data.

PACS number(s): 13.20.He, 12.39.Ki, 13.20.Fc

I. INTRODUCTION

Semileptonic decays of heavy mesons provide an important tool to investigate quark dynamics and to determine Cabibbo-Kobayashi-Maskawa (CKM) matrix elements. Hadron dynamics is contained in form factors, which are Lorentz-invariant functions of q^2, the square of the momentum transfer. These form factors cannot be calculated from first principles of QCD yet. Thus various potential models, sum rules, and lattice calculations have been proposed [1–6]. Recently considerable progress has been achieved in describing heavy meson decays by the use of heavy quark effective theory (HQET) [7]. It has been found that in the limit of infinitely heavy b and c quarks their mass and spin decouple from the dynamics of the decay and the description of a process such as $B \to D l\nu_l$ is strongly simplified. For D decays HQET predictions are less useful, because in this case symmetry-breaking corrections appear to be rather large. As shown in [8], the symmetry-breaking corrections may increase up to 30%. It is also important to note that, since B and D mesons contain light quarks, relativistic effects are quite significant and a consistent relativistic description of the heavy-light quark system is necessary.

Our relativistic quark model (RQM) has some features that make it attractive and reliable for the description of heavy mesons. First, the the RQM provides a consistent scheme for calculation of all relativistic corrections and allows for the heavy quark $1/m_Q$ expansion. Secondly, it has been found [9] that the general structure of leading, next-to-leading, and second order $1/m_Q$ corrections in the RQM is in accord with the predictions of HQET. The HQET and QCD impose some rigid constraints on the parameters of the long-range confining potential of our model. This gives an additional motivation for the choice of the main parameters of the RQM and leads us to the conclusion that the confining quark-antiquark potential in mesons is predominantly a Lorentz vector (with the Pauli term), while the scalar potential is anticonfining and helps to reproduce the initial nonrelativistic potential. This model has been applied to calculations of meson mass spectra [10], radiative decay widths [11], pseudoscalar decay constants [12], and rare radiative [13] and nonleptonic [14] decay rates. Semileptonic decays of B and D mesons have been considered in our model in [15]. Here we refine our previous analysis with a more complete account of relativistic effects and HQET constraints. We also consider exclusive decay spectra and q^2 dependence of form factors.

In Sec. II we briefly describe the RQM. Section III is devoted to the calculation of form factors and semileptonic branching ratios and contains analytical expressions and numerical results for the differential distributions for decays into pseudoscalar as well as vector final states. We give our conclusions in Sec. IV.

II. RELATIVISTIC QUARK MODEL

Our model is based on the quasipotential approach in quantum field theory [16]. A quark-antiquark bound system with mass M and relativistic momentum $\mathbf{p}$ in the center of mass system is described by a single-time quasipotential wave function $\Psi_M(\mathbf{p})$, projected onto positive-energy states. This wave function satisfies the quasipotential equation

$$\left[M - (\mathbf{p}^2 + m_1^2)^{1/2} - (\mathbf{p}^2 + m_2^2)^{1/2}\right] \Psi_M(\mathbf{p}) = \int \frac{d^3\mathbf{q}}{(2\pi)^3} V(\mathbf{p}, \mathbf{q}; M) \Psi_M(\mathbf{q}). \quad (1)$$

The quasipotential equation (1) can be transformed into a local Schrödinger-like equation [17]

$$\left[\frac{b^2(M)}{2\mu_R} - \frac{\mathbf{p}^2}{2\mu_R}\right] \Psi_M(\mathbf{p}) = \int \frac{d^3\mathbf{q}}{(2\pi)^3} V(\mathbf{p}, \mathbf{q}; M) \Psi_M(\mathbf{q}), \quad (2)$$

where the relativistic reduced mass is

$$\mu_R = \frac{E_1 E_2}{E_1 + E_2} = \frac{M^4 - (m_1^2 - m_2^2)^2}{4M^3},$$
$$E_1 = \frac{M^2 - m_2^2 + m_1^2}{2M}, \quad E_2 = \frac{M^2 - m_1^2 + m_2^2}{2M}, \tag{3}$$
$$E_1 + E_2 = M,$$

and the square of the relative momentum on the mass shell is

$$b^2(M) = \frac{[M^2 - (m_1 + m_2)^2]\,[M^2 - (m_1 - m_2)^2]}{4M^2}, \tag{4}$$

where $m_{1,2}$ are the quark masses.

Now it is necessary to construct the quasipotential $V(\mathbf{p}, \mathbf{q}; M)$ of the quark-antiquark interaction. As is well known from QCD, in view of the property of asymptotic freedom the one-gluon exchange potential gives the main contribution at short distances. With increase of the distance the long-range confining interaction becomes dominant. At present the form of this interaction cannot be established in the framework of QCD. The most general kernel of the $q\bar{q}$ interaction, corresponding to the requirements of Lorentz invariance and of P and T invariance, contains [18, 19] scalar, pseudoscalar, vector, axial-vector, and tensor parts. The analysis carried out in [10,18] has shown that the leading contributions to the confining part of the potential should have a vector and scalar structure. On the basis of these arguments we have assumed that the effective interaction is the sum of the one-gluon exchange term and the mixture of long-range vector with scalar potentials. We have also assumed that at large distances quarks acquire universal nonperturbative anomalous chromomagnetic moments and thus the vector long-range potential contains the Pauli interaction. The quasipotential is defined by [10]

$$V(\mathbf{p}, \mathbf{q}; M) = \bar{u}_1(p)\bar{u}_2(-p)\left[\tfrac{4}{3}\alpha_s D_{\mu\nu}(\mathbf{k})\gamma_1^\mu \gamma_2^\nu + V_{\rm conf}^V(\mathbf{k})\Gamma_1^\mu \Gamma_{2;\mu} + V_{\rm conf}^S(\mathbf{k})\right] \times u_1(q)u_2(-q), \tag{5}$$

where α_s is the QCD coupling constant, $D_{\mu\nu}$ is the gluon propagator, γ_μ and $u(p)$ are the Dirac matrices and spinors, $\mathbf{k} = \mathbf{p} - \mathbf{q}$, Γ_μ is the effective vector vertex at large distances:

$$\Gamma_\mu(\mathbf{k}) = \gamma_\mu + \frac{i\kappa}{2m}\sigma_{\mu\nu}k^\nu, \tag{6}$$

and κ is the anomalous chromomagnetic quark moment.

The complete expression for the quasipotential obtained from (5) and (6) taking into account the relativistic corrections of order v^2/c^2 can be found in [10]. In the nonrelativistic limit vector and scalar confining potentials reduce to

$$V_{\rm conf}^V(r) = (1 - \varepsilon)(Ar + B), \quad V_{\rm conf}^S(r) = \varepsilon(Ar + B), \tag{7}$$

reproducing $V_{\rm nonrel}^{\rm conf}(r) = V_{\rm conf}^S + V_{\rm conf}^V = Ar + B$, where ε is the mixing coefficient.

All the parameters of our model, quark masses, the parameters of the linear confining potential A and B, mixing coefficient ε, and anomalous chromomagnetic quark moment κ, were originally fixed from the analysis of meson masses [10] and radiative decays [11]. The quark masses, m_b= 4.88 GeV, m_c= 1.55 GeV, m_s= 0.50 GeV, $m_{u,d}$= 0.33 GeV, and parameters of the linear potential, A= 0.18 GeV^2, B = −0.30 GeV, have standard values for quark models. The value of the mixing coefficient of vector and scalar confining potentials $\varepsilon = -0.9$ has been chosen primarily from consideration of meson radiative decays, which are rather sensitive to the Lorentz structure of the confining potential [11]. The universal anomalous chromomagnetic moment of quarks, $\kappa = -1$, has been fixed from analysis of the fine splitting of heavy quarkonia ^3P_J states [10].

Recently, in the framework of the RQM, the $1/m_Q$ expansion of the matrix elements of weak currents between pseudoscalar and vector heavy meson states has been performed [9]. It has been found that the heavy quark symmetry (in the case of infinite m_Q) relations are reproduced in the RQM without any adjustment of the model parameters. The constraints emerge only in case heavy quark symmetry is violated, i.e., for finite m_Q. The particular structure of $1/m_Q$ corrections up to the second order predicted by HQET can be reproduced in the RQM only with some specific values of κ and ε. The analysis of the first order corrections [9] allowed one to fix $\kappa = -1$, while from consideration of the second order corrections the result has been obtained that the mixing parameter ε should be $\varepsilon = -1$. Thus HQET, and hence QCD, imposes strong constraints on the parameters of the long-range confining potential. The obtained value of ε is very close to the previous one, determined phenomenologically from radiative decays [11], and the value of κ coincides with the result obtained from the mass spectra [10]. Therefore there is an important QCD and HQET motivation for the choice of the main parameters of our model: $\varepsilon = -1$, $\kappa = -1$.

III. EXCLUSIVE SEMILEPTONIC DECAY

A. Form factors and decay widths

For the semileptonic decay $B \to A(A^*)l\nu_l$ of the pseudoscalar meson B into the pseudoscalar (vector) meson A (A^*) the differential width can be written as

$$d\Gamma(B \to A(A^*)l\nu_l) = \frac{1}{2M_B} \mid \mathcal{A}(B \to A(A^*)l\nu_l) \mid^2 d\Phi, \tag{8}$$

where

$$d\Phi = (2\pi)^4 \delta^{(4)}(p_B - p_l - p_{\nu_l} - p_A) \prod_i \frac{d^3 p_i}{(2\pi)^3 2E_i}, \quad i = A, l, \nu_l, \tag{9}$$

p_B is the four-momentum of the initial meson, p_A is the four-momentum of the final meson, and p_l and p_{ν_l} are the four-momenta of the lepton and neutrino, respectively.

The relevant transition amplitude looks like

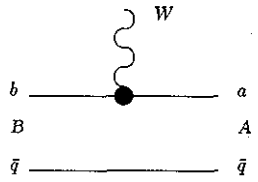

FIG. 1. Lowest order vertex function.

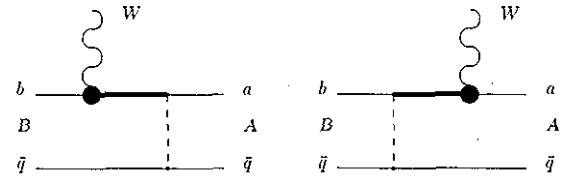

FIG. 2. Vertex function with account of the quark interaction. Dashed line corresponds to the effective potential (5). Bold line denotes the negative-energy part of the quark propagator.

$$\mathcal{A}(B \to A(A^*)l\nu_l) = \langle A(A^*)l\nu_l|H_{\rm eff}|B\rangle = \frac{G_F}{\sqrt{2}}V_{ab}L_\mu H^\mu, \tag{10}$$

where

$$H_{\rm eff} = \frac{G_F}{\sqrt{2}}J^\mu_{\rm hadron}J_{{\rm lepton};\mu} \tag{11}$$

and V_{ab} is the CKM matrix element connected with the $b \to a$ transition.

The leptonic L_μ and hadronic H_μ currents are defined by

$$L_\mu = \bar{l}\gamma_\mu(1-\gamma_5)\nu_l, \tag{12}$$

$$H_\mu = \langle A(A^*)|\bar{a}\gamma_\mu(1-\gamma_5)b|B\rangle; \tag{13}$$

the initial meson B has the quark structure $(b\bar{q})$ and the final meson A (A^*) has the quark structure $(a\bar{q})$.

The matrix element of the hadron current can be expressed in terms of Lorentz-invariant form factors.

(a) For the $0^- \to 0^-$ transition $B \to Al\nu_l$,

$$\langle A(p_A)|J^V_\mu|B(p_B)\rangle = f_+(q^2)(p_A+p_B)_\mu + f_-(q^2)(p_B-p_A)_\mu; \tag{14}$$

(b) for the $0^- \to 1^-$ transition $B \to A^*l\nu_l$,

$$\langle A^*(p_A,e)|J^V_\mu|B(p_B)\rangle = i\frac{V(q^2)}{M_A+M_B}\epsilon_{\mu\nu\rho\sigma}e^{*\nu}(p_A+p_B)^\rho(p_B-p_A)^\sigma; \tag{15}$$

$$\langle A^*(p_A,e)|J^A_\mu|B(p_B)\rangle = (M_A+M_B)A_1(q^2)e^*_\mu - \frac{A_2(q^2)}{M_A+M_B}(e^*p_B)(p_A+p_B)_\mu + \frac{A_3(q^2)}{M_A+M_B}(e^*p_B)(p_B-p_A)_\mu; \tag{16}$$

where $q = p_B - p_A$, $J^V_\mu = (\bar{a}\gamma_\mu b)$ and $J^A_\mu = (\bar{a}\gamma_\mu\gamma_5 b)$ are the vector and axial parts of the weak current, and e_μ is the polarization vector of the A^* meson.

Since $q = p_l + p_{\nu_l}$, the terms proportional to q_ν, i.e., f_- and A_3, give contributions proportional to the lepton masses and do not influence significantly the transition amplitude, except for the case of the heavy, τ lepton, and thus will not be considered.

The matrix element of the local current J between bound states in the quasipotential method has the form [20]

$$\langle A|J_\mu(0)|B\rangle = \int\frac{d^3\mathbf{p}d^3\mathbf{q}}{(2\pi)^6}\bar{\Psi}_A(\mathbf{p})\Gamma_\mu(\mathbf{p},\mathbf{q})\Psi_B(\mathbf{q}), \tag{17}$$

where $\Gamma_\mu(\mathbf{p},\mathbf{q})$ is the two-particle vertex function and $\Psi_{A,B}$ are meson wave functions projected onto the positive-energy quark states.

In the case of semileptonic decays $J_\mu = J_{{\rm hadron};\mu} = J^V_\mu - J^A_\mu$ is the weak quark current and in order to calculate its matrix element between meson states it is necessary to consider the contributions to Γ from Figs. 1 and 2. The vertex functions obtained from these diagrams look like

$$\Gamma^{(1)}_\mu(\mathbf{p},\mathbf{q}) = \bar{u}_a(p_1)\gamma_\mu(1-\gamma_5)u_b(q_1)(2\pi)^3\delta(\mathbf{p}_2-\mathbf{q}_2), \tag{18}$$

and

$$\Gamma^{(2)}_\mu(\mathbf{p},\mathbf{q}) = \bar{u}_a(p_1)\bar{u}_q(p_2)\Big[\gamma_{1\mu}(1-\gamma_1^5)\frac{\Lambda_b^{(-)}(\mathbf{k})}{\varepsilon_b(k)+\varepsilon_b(p_1)}\gamma_1^0V(\mathbf{p}_2-\mathbf{q}_2) + V(\mathbf{p}_2-\mathbf{q}_2)\frac{\Lambda_a^{(-)}(\mathbf{k}')}{\varepsilon_a(k')+\varepsilon_a(q_1)}\gamma_1^0\gamma_{1\mu}(1-\gamma_1^5)\Big]u_b(q_1)u_q(q_2), \tag{19}$$

where $\mathbf{k} = \mathbf{p}_1 - \mathbf{\Delta}$, $\mathbf{k}' = \mathbf{q}_1 + \mathbf{\Delta}$, $\mathbf{\Delta} = \mathbf{p}_B - \mathbf{p}_A$, $\varepsilon(p) = (m^2+\mathbf{p}^2)^{1/2}$, and

$$\Lambda^{(-)}(p) = \frac{\varepsilon(p) - (m\gamma^0 + \gamma^0\vec{\gamma}\mathbf{p})}{2\varepsilon(p)}.$$

As one can see, the form of relativistic corrections resulting from $\Gamma^{(2)}_\mu(\mathbf{p},\mathbf{q})$ is explicitly dependent on the Lorentz structure of the quark-antiquark potential.

Our previous analysis of the semileptonic $B \to D(D^*)$ and $D \to K(K^*)$ transitions [15] was based on the as-

sumption that we could expand (19) up to the order $\mathbf{p}^2/m^2$ with respect to both b and a quarks. This assumption proved to be quite adequate in the case of $B \to Dl\nu_l$ where both b and c quarks are heavy. However, the final s quark is not heavy enough. It would be more accurate not to expand $\Gamma_\mu^{(2)}(\mathbf{p},\mathbf{q})$ at all, but one should do it in order to perform one of the integrations in (17). Our statement is that more reliable results for semileptonic $D \to K$ decays can be obtained by using a $\mathbf{p}^2/\varepsilon_a^2(p)$ expansion instead of $\mathbf{p}^2/m^2$ in (19).

It is also necessary to take into account that the wave function of the final A meson $\Psi_{A,\mathbf{p}_A}(\mathbf{p})$ is connected with the one in the A rest frame $\Psi_{A,0}(\mathbf{p})$ as follows [20]:

$$\Psi_{A,\mathbf{p}_A}(\mathbf{p}) = D_a^{1/2}(R^W_{L_{\mathbf{p}_A}})D_q^{1/2}(R^W_{L_{\mathbf{p}_A}})\Psi_{A,0}(\mathbf{p}), \quad (20)$$

where $D^{1/2}(R)$ is the well-known rotation matrix and R^W is the Wigner rotation.

The meson functions in the rest frame have been calculated [21] by numerical solution of the quasipotential equation (2). However, it is more convenient to use analytical expressions for meson wave functions. Examination of the numerical results for the ground state wave functions of mesons containing at least one light quark has shown that they can be well approximated by the Gaussian functions

$$\Psi_M(\mathbf{p}) \equiv \Psi_{M,0}(\mathbf{p}) = \left(\frac{4\pi}{\beta_M^2}\right)^{3/4} \exp\left(-\frac{\mathbf{p}^2}{2\beta_M^2}\right), \quad (21)$$

with the deviation less than 5%.

The parameters are

$$\beta_B = 0.41\,\text{GeV}, \quad \beta_K = \beta_{K^*} = 0.33\,\text{GeV},$$
$$\beta_\phi = 0.36\,\text{GeV}, \quad \beta_D = 0.38\,\text{GeV}, \quad \beta_{D_s} = 0.44\,\text{GeV}. \quad (22)$$

In the B meson rest frame Eqs. (14)–(16) can be written in the three-dimensional form.

(a) For the $0^- \to 0^-$ transition $B \to Al\nu_l$,

$$\langle A(p_A)|J_0^V|B(p_B)\rangle = f_+(q^2)(M_B + E_A) + f_-(q^2)(M_B - E_A), \quad (23)$$

$$\langle A(p_A)|\mathbf{J}^V|B(p_B)\rangle = [f_-(q^2) - f_+(q^2)]\boldsymbol{\Delta}, \quad (24)$$

(b) for the $0^- \to 1^-$ transition $B \to A^* l\nu_l$,

$$\langle A^*(p_A,e)|J_0^V|B(p_B)\rangle = i\frac{V(q^2)}{M_A+M_B}\epsilon_{0\nu\rho\sigma}\tilde{e}^{*\nu}(p_A+p_B)^\rho(p_B-p_A)^\sigma = 0, \quad (25)$$

$$\langle A^*(p_A,e)|\mathbf{J}^V|B(p_B)\rangle = i\frac{2M_B}{M_A+M_B}V(q^2)[\tilde{\mathbf{e}}^*\boldsymbol{\Delta}], \quad (26)$$

$$\langle A^*(p_A,e)|J_0^A|B(p_B)\rangle = \tilde{e}_0^*\Big(A_1(q^2)(M_A+M_B) - A_2(q^2)\frac{M_B}{M_A+M_B}(M_B+E_A) + A_3(q^2)\frac{M_B}{M_A+M_B}(M_B-E_A)\Big), \quad (27)$$

$$\langle A^*(p_A,e)|\mathbf{J}^A|B(p_B)\rangle = A_1(q^2)(M_A+M_B)\tilde{\mathbf{e}} - \boldsymbol{\Delta}\tilde{e}_0^*\frac{M_B}{M_A+M_B} \times [A_2(q^2)+A_3(q^2)], \quad (28)$$

where $e_\mu = (0,\mathbf{e})$ is the polarization vector of the A^* meson in its rest frame and $\tilde{e}_\mu$ is the vector obtained from e_μ by the Lorentz transformation L_Δ:

$$\tilde{e}_\mu = L_\Delta e_\mu. \quad (29)$$

The components of $\tilde{e}_\mu$ look like

$$\tilde{e}_0 = \frac{\mathbf{e}\boldsymbol{\Delta}}{M_A}, \quad \tilde{\mathbf{e}} = \mathbf{e} + \frac{\boldsymbol{\Delta}(\boldsymbol{\Delta}\mathbf{e})}{M_A(E_A+M_A)} = \mathbf{e} + \tilde{e}_0\frac{\boldsymbol{\Delta}}{E_A+M_A}. \quad (30)$$

Equations (23), (24), and (25)–(28) determine the form factors f_+, f_-, and V, A_1, A_2, and A_3, respectively.

Substituting the vertex functions (18) and (19), taking account of wave function transformation (20) and quasipotential equation (1), in the matrix element (17) and using Eqs. (23), (24), and (25)–(28) we get the following expressions at the $q^2 = q^2_{\max} = (M_B - M_A)^2$ point:

$$f_+(q^2_{\max}) = f_+^{(1)}(q^2_{\max}) + \varepsilon f_{+S}^{(2)}(q^2_{\max}) + (1-\varepsilon)f_{+V}^{(2)}(q^2_{\max}), \quad (31)$$

$$A_1(q^2_{\max}) = A_1^{(1)}(q^2_{\max}) + \varepsilon A_{1S}^{(2)}(q^2_{\max}) + (1-\varepsilon)A_{1V}^{(2)}(q^2_{\max}), \quad (32)$$

$$A_2(q^2_{\max}) = A_2^{(1)}(q^2_{\max}) + \varepsilon A_{2S}^{(2)}(q^2_{\max}) + (1-\varepsilon)A_{2V}^{(2)}(q^2_{\max}), \quad (33)$$

$$V(q^2_{\max}) = V^{(1)}(q^2_{\max}) + \varepsilon V_S^{(2)}(q^2_{\max}) + (1-\varepsilon)V_V^{(2)}(q^2_{\max}), \quad (34)$$

where $f_+^{(1)}$, $f_{+S,V}^{(2)}$, $A_{1,2}^{(1)}$, $A_{1S,V}^{(2)}$, $A_{2S,V}^{(2)}$, $V^{(1)}$, and $V_{S,V}^{(2)}$ are given in Appendix A. In (31)–(34) indices (1) and (2) correspond to the diagrams in Figs. 1 and 2, and S and V correspond to the scalar and vector potentials of quark interaction.

Now our concern is to find the q^2 dependence of the form factors. The components of axial and vector currents can be expressed in terms of two functions $F_1(\boldsymbol{\Delta})$ and $F_2(\boldsymbol{\Delta})$, $\boldsymbol{\Delta} = \mathbf{p}_B - \mathbf{p}_A$:

$$J_0^V(\boldsymbol{\Delta}) = F_2(\boldsymbol{\Delta}), \quad (35)$$

$$\mathbf{J}^V(\boldsymbol{\Delta}) = \frac{\boldsymbol{\Delta} + i[\mathbf{e}^*\boldsymbol{\Delta}]}{2m_a}F_1(\boldsymbol{\Delta}), \quad (36)$$

$$J_0^A(\boldsymbol{\Delta}) = \frac{(\mathbf{e}^*\boldsymbol{\Delta})}{2m_a}F_1(\boldsymbol{\Delta}), \quad (37)$$

$$\mathbf{J}^A(\boldsymbol{\Delta}) = \mathbf{e}^*F_2(\Delta). \quad (38)$$

The functions F_1 and F_2 arise from the lower and the upper components of Dirac spinors;

$$u_a^\lambda(p) = \left(\frac{\varepsilon_a(p)+m_a}{2\varepsilon_a(p)}\right)^{1/2}\begin{pmatrix}1\\ \frac{\vec{\sigma}\mathbf{p}}{\varepsilon_a(p)+m_a}\end{pmatrix}\chi^\lambda, \quad (39)$$

and are equal to

$$F_1(\mathbf{\Delta}) = \frac{2m_a}{\varepsilon_a(\mathbf{q}+\mathbf{\Delta})+m_a} \times \left(\frac{\varepsilon_a(\mathbf{q}+\mathbf{\Delta})+m_a}{2\varepsilon_a(\mathbf{q}+\mathbf{\Delta})}\right)^{1/2} \sqrt{\frac{E_A}{M_A}}, \quad (40)$$

$$F_2(\mathbf{\Delta}) = \left(\frac{\varepsilon_a(\mathbf{q}+\mathbf{\Delta})+m_a}{2\varepsilon_a(\mathbf{q}+\mathbf{\Delta})}\right)^{1/2} \sqrt{\frac{E_A}{M_A}}. \quad (41)$$

Near $q^2 = q^2_{\max}$ they can be written as

$$F_1(\mathbf{\Delta}) = \frac{\sqrt{2}(1+\mathbf{\Delta}^2/M_A^2)^{1/2}}{\left(1+\mathbf{\Delta}^2/m_a^2+\sqrt{1+\mathbf{\Delta}^2/m_a^2}\right)^{1/2}}, \quad (42)$$

$$F_2(\mathbf{\Delta}) = \frac{1}{\sqrt{2}}\left(1+\frac{1}{\sqrt{1+\mathbf{\Delta}^2/m_a^2}}\right)^{1/2}\left(1+\frac{\mathbf{\Delta}^2}{M_A^2}\right)^{1/2}. \quad (43)$$

The dependence of the form factors on the momentum transfer is fixed by extrapolating their behavior near the $q^2 = q^2_{\max}$ ($\mathbf{\Delta} = \mathbf{0}$) point over the kinematically allowed region:

$$f_+(\mathbf{\Delta}) = f_+(0)I(\mathbf{\Delta})F_1(\mathbf{\Delta}), \quad (44)$$

$$A_1(\mathbf{\Delta}) = A_1(0)I(\mathbf{\Delta})F_2(\mathbf{\Delta}), \quad (45)$$

$$A_2(\mathbf{\Delta}) = A_2(0)I(\mathbf{\Delta})F_1(\mathbf{\Delta}), \quad (46)$$

$$V(\mathbf{\Delta}) = V(0)I(\mathbf{\Delta})F_1(\mathbf{\Delta}), \quad (47)$$

where

$$I(\mathbf{\Delta}) = \int \frac{d^3\mathbf{p}}{(2\pi)^3}\bar{\Psi}_A\left(\mathbf{p}+\frac{2\varepsilon_q}{E_A+M_A}\mathbf{\Delta}\right)\Psi_B(\mathbf{p}). \quad (48)$$

Introducing the variable

$$w \equiv v_A v_B = \frac{M_B^2+M_A^2-q^2}{2M_AM_B}, \quad (49)$$

where v_A and v_B are meson velocities, and taking into account that

$$\mathbf{\Delta}^2 = (\mathbf{p}_B-\mathbf{p}_A)^2 = \frac{(M_B^2+M_A^2-q^2)^2}{4M_B^2} - M_A^2 = M_A^2(w^2-1), \quad (50)$$

we can rewrite (44)–(47) in the form

$$f_+(w) = f_+(1)I(w)\left(\frac{2}{w+1}\right)^{1/2}, \quad (51)$$

$$A_1(w) = A_1(1)I(w)\left(\frac{w+1}{2}\right)^{1/2}, \quad (52)$$

$$A_2(w) = A_2(1)I(w)\left(\frac{2}{w+1}\right)^{1/2}, \quad (53)$$

$$V(w) = V(1)I(w)\left(\frac{2}{w+1}\right)^{1/2}. \quad (54)$$

Substitution of the Gaussian wave functions (21) in (48) results in

$$I(w) = \exp\left(-\frac{2\bar{\Lambda}^2_{\mathrm{RQM}}}{\beta^2_{M_A}+\beta^2_{M_B}}\frac{w-1}{w+1}\right)I(1), \quad (55)$$

where $\bar{\Lambda}_{\mathrm{RQM}} = \langle\varepsilon_q\rangle$ is the mean value of light quark energy inside the meson. In our model $\bar{\Lambda}_{\mathrm{RQM}}$ corresponds to the HQET parameter $\bar{\Lambda} = M - m_Q$, which determines the energy carried by light degrees of freedom, and is found to be [9] $\bar{\Lambda}_{\mathrm{RQM}} = 0.54 \pm 0.03$ GeV.

In the limit of infinitely heavy b and a quarks the w dependence of Eqs. (51)–(55) is determined by the Isgur-Wise function of our model,

$$\xi(w) = \left(\frac{2}{w+1}\right)^{1/2}\exp\left(-\frac{\bar{\Lambda}^2_{\mathrm{RQM}}}{\beta^2}\frac{w-1}{w+1}\right) \quad (56)$$

and the ratios of form factors satisfy all constraints imposed by HQET [7].

Using (31)–(34) and (A1)–(A10) we have calculated form factors for the $B \to D(D^*)l\nu_l$, $D \to K(K^*)l\nu_l$, and $D_s \to \varphi l\nu_l$ exclusive decays. First, these form factors were calculated at the $q^2 = q^2_{\max}$ point by using the wave functions obtained by the numerical solution of the quasipotential equation [21]. Then they were extrapolated to $q^2 = 0$ with the (51)–(55) dependence. The theoretical uncertainty in the calculation of the form factors at $q^2 = q^2_{\max}$ results from the terms of order v^4/c^4 and does not exceed 1% for $B \to D$ and 4% for $D \to K$ decays. The main theoretical errors in the form factor values at $q^2 = 0$ as well as in the decay widths come from the q^2 dependence of the form factors (51)–(55), which has been obtained by analytical approximation of the wave functions by Gaussians (21). The analysis has shown that the total theoretical uncertainty of the RQM calculations for form factors and decay widths is less than 10% for $D \to K$ and 7% for $B \to D$ semileptonic decays.

The results obtained in our model for $D \to K(K^*)l\nu_l$ are compared with appropriate experimental data and various model predictions in Table I. The new values of the form factors for $D \to K(K^*)l\nu_l$ are somewhat larger than our previous results [15] because of a more consistent relativistic treatment of the s quark and a slight change in the value of the mixing coefficient ε. Note that, while most other quark models agree with the experimental determination of $V(0)$, but fail to predict $A_1(0)$ and/or $A_2(0)$, our model predicts correct values of $A_1(0)$ and $A_2(0)$, but gives too low a value of $V(0)$. The reason for that is not clear. However, the contribution from the form factor $V(0)$ in the total width is kinematically suppresed. So, despite the above mentioned discrepancy, we have obtained the $D \to K^*l\nu_l$ width in accord with experimental data.

The ratios of form factors

$$R_2 = \left(1-\frac{q^2}{(M_{A^*}+M_B)^2}\right)A_2(q^2)/A_1(q^2)$$

and

$$R_V = \left(1-\frac{q^2}{(M_{A^*}+M_B)^2}\right)V(q^2)/A_1(q^2)$$

are given in Table II. It is important to note that the theoretical error in the form factor ratios is less than that in their values at the point $q^2 = 0$. Really, most of the errors connected with the q^2 dependence in (51)–(55)

TABLE I. Theoretical predictions and experimental data for form factors in $D \to Kl\nu_l$ and $D \to K^* l\nu_l$.

Ref.	$f_+(0)$	$V_0(0)$	$A_1(0)$	$A_2(0)$
Expt. average [23]	$0.75 \pm 0.02 \pm 0.02$	1.1 ± 0.2	0.56 ± 0.04	0.40 ± 0.08
Theory				
RQM	0.73 ± 0.07	0.62 ± 0.06	0.63 ± 0.06	0.43 ± 0.04
ISGW [1]	0.82	1.1	0.8	0.8
BSW [2]	0.76	1.3	0.88	1.2
AW [3]	0.7	1.5	0.8	0.6
BKS [4]	$0.9 \pm 0.08 \pm 0.21$	$1.4 \pm 0.5 \pm 0.5$	$0.8 \pm 0.1 \pm 0.3$	$0.6 \pm 0.1 \pm 0.2$
LMMS [5]	0.63 ± 0.08	0.9 ± 0.1	0.53 ± 0.03	0.2 ± 0.2
BBD [6]	0.6	1.1	0.5	0.6

are canceled out in R_2 and R_V. Thus, according to our analysis, the errors in R_2 and R_V do not exceed 5%.

The obtained branching ratios are

$$B(D^0 \to K^{*-} e^+ \nu_e) = (1.9 \pm 0.2)\%$$

$$\text{for } \tau_{D^0} = 0.415 \times 10^{-12} \text{ s},$$

$$B(D^+ \to \bar{K}^{*0} e^+ \nu_e) = (4.9 \pm 0.5)\%$$

$$\text{for } \tau_{D^+} = 1.060 \times 10^{-12} \text{ s},$$

to be compared with the experimental average data [23]

$$B^{\text{expt}}(D^0 \to K^{*-} e^+ \nu_e) = (2.0 \pm 0.4)\%,$$

$$B^{\text{expt}}(D^+ \to \bar{K}^{*0} e^+ \nu_e) = (4.8 \pm 0.4)\%.$$

The ratio $\Gamma(D \to K^* e\nu_e)/\Gamma(D \to Ke\nu_e)$ and the ratio of the longitudinal and transverse decay widths Γ_L/Γ_T also agree well with experiment (see Table III).

For the $D_s \to \varphi l\nu_l$ decay form factors our predictions are

$$A_1(0) = 0.63 \pm 0.06, \quad A_2(0) = 0.35 \pm 0.04,$$
$$V(0) = 1.06 \pm 0.09.$$

TABLE II. Calculated and measured $D \to K^* l\nu_l$ form factor ratios $R_2(0) = A_2(0)/A_1(0)$ and $R_V(0) = V(0)/A_1(0)$.

Ref.	$R_2(0)$	$R_V(0)$
Experiment		
E691 [31]	$0.0 \pm 0.5 \pm 0.2$	$2.0 \pm 0.6 \pm 0.3$
E653 [32]	$0.82^{+0.22}_{-0.23} \pm 0.11$	$2.00^{+0.34}_{-0.32} \pm 0.16$
E687 [33]	$0.78 \pm 0.18 \pm 0.10$	$1.74 \pm 0.27 \pm 0.28$
Expt. average [23]	0.73 ± 0.15	1.89 ± 0.25
Theory		
RQM	0.68	0.98
ISGW [1]	1.0	1.37
BSW [2]	1.36	1.48
AW [3]	0.75	1.87
BKS [4]	$0.7 \pm 0.16 \pm 0.17$	$1.99 \pm 0.22 \pm 0.33$
LMMS [5]	0.4 ± 0.4	1.6 ± 0.2
BBD [6]	1.2	2.2

As the experiment provides us with R_2 and R_V ratios for $D_s \to \varphi l\nu_l$, we compare them with predicted values in Table IV. It is not clear why the experimental ratio R_2 for $D_s \to \varphi l\nu_l$ differs so greatly from that for $D \to K^* l\nu_l$. In the RQM we get approximately equal ratios R_2 for both decays, because the general structure and the signs of the potential-dependent corrections in (31)–(34) are almost the same. It can be expected that the experimental results for the $D_s \to \varphi l\nu_l$ form factor ratios will change in the future. Anyway, the experimental uncertainties are still too large to conclude that there is a serious discrepancy between the RQM and the experimental data in this case.

For the $D_s \to \varphi l\nu_l$ branching ratio we have $B(D_s \to \varphi l\nu_l) = (2.5 \pm 0.3)\%$, while the experiment gives $B^{\text{expt}}(D_s \to \varphi l\nu_l) = (1.88 \pm 0.29)\%$ [23].

In $B \to D^* l\nu_l$ decay, since both b and c quarks are heavy, relativistic corrections are not so significant, but the Lorentz structure of the quark-antiquark potential has an important influence on the values of the form factors. We have found our results for R_2 and R_V to be in good agreement with the experimental data [24] and HQET-based predictions [26]. Measurements and predictions for the ratios of the form factors for $B \to D^* l\nu_l$, evaluated at $q^2 = q^2_{\max}$, are shown in Table V. We have obtained the following results for $B \to D^* l\nu_l$ and $B \to Dl\nu_l$ branching ratios:

$$B(B \to D^* l\nu_l) = (33.8 \pm 2.5) \times |V_{bc}|^2,$$

$$B(B \to Dl\nu_l) = (14.8 \pm 1.5) \times |V_{bc}|^2,$$

for $\tau_{B^0} = 1.5 \times 10^{-12}$ s. They should be compared to the

TABLE III. The ratios $\Gamma(D \to K^* l\nu_l)/\Gamma(D \to Kl\nu_l)$ and Γ_L/Γ_T in comparison with the experimental data.

Ref.	$\Gamma(K^*)/\Gamma(K)$	Γ_L/Γ_T
RQM	0.65	1.05
Experiment		
Expt. average [23]		1.23 ± 0.13
E691 [31]		$1.8^{+0.6}_{-0.4} \pm 0.3$
E653 [32]		$1.18 \pm 0.18 \pm 0.08$
E687 [33]		$1.20 \pm 0.13 \pm 0.13$
CLEO [34]	$0.60 \pm 0.09 \pm 0.07$	
CLEO [34]	$0.65 \pm 0.09 \pm 0.10$	

TABLE IV. Measured and calculated ratios of form factors in $D_s \to \phi l \nu_l$.

Ref.	$R_2(0)$	$R_V(0)$
Expt. average [23]	1.8 ± 0.5	2.0 ± 0.7
CLEO [36]	$1.4 \pm 0.5 \pm 0.3$	$0.9 \pm 0.6 \pm 0.3$
E653 [37]	$2.1^{+0.6}_{-0.5} \pm 0.2$	$2.3^{+1.1}_{-0.9} \pm 0.4$
Theory		
RQM	0.55	0.94
BKS [4]	$2.0 \pm 0.19 \pm 0.23$	$0.78 \pm 0.08 \pm 0.15$
LMMS [5]	1.65 ± 0.2	0.33 ± 0.36

experimental data:

$$B(B^0 \to D^- e^+ \nu_e) = (2.0 \pm 0.7 \pm 0.6)\% \quad \text{ARGUS [27]},$$

$$B(B^0 \to D^- e^+ \nu_e) = (1.8 \pm 0.6 \pm 0.3)\% \quad \text{CLEO-I [28]},$$

$$B(B^0 \to D^{*-} e^+ \nu_e) = (4.7 \pm 0.5 \pm 0.5)\% \quad \text{ARGUS [29]},$$

$$B(B^0 \to D^{*-} e^+ \nu_e) = (4.0 \pm 0.4 \pm 0.6)\% \quad \text{CLEO-I[28,30]}.$$

As a result we can extract the value of the CKM matrix element V_{cb},

$$|V_{cb}| = 0.036 \pm 0.001 \pm 0.004,$$

where the first error represents the theoretical uncertainties and the second one arises from the errors in the experimental measurments.

B. Differential distributions

The differential decay rate [22] can be expressed in terms of two dimensionless variables $x = E_l/M_B$ and $w = v_A v_B$, where E_l is the lepton energy,

TABLE V. Predicted and measured ratios of form factors in $B \to D^* l \nu_l$ at $q^2 = q^2_{\max}$.

Ref.	$R_2(q^2_{\max})$	$R_V(q^2_{\max})$
Experiment		
CLEO [24]	0.79 ± 0.28	1.32 ± 0.62
Theory		
RQM	0.92	1.39
ISGW [1]	0.91	1.01
WSB [2]	0.85	0.91
HQET(the leading order) [25]	1.00	1.00
HQET based [26]	0.91	1.39
HQET(Neubert) [7]	0.79	1.35
LNN [38]	0.8	

$$\frac{d^2\Gamma}{dx\,dw} = \frac{|V_{ab}|^2 G_F^2 M_B^5}{32\pi^3}\left\{\left(\frac{2M_A}{M_B}w - 1 - \rho\right) \times \left[W_1(w) - 2W_3(w)\left(1 - 2x - \frac{M_A}{M_B}w\right)\right] + 2W_2(w)\left(\rho + (1-2x)^2 - \frac{2M_A}{M_B}w(1-2x)\right)\right\}, \tag{57}$$

Here $W_{1,2,3}(w)$ are connected with semileptonic form factors.

(a) For the $0^- \to 0^-$ transition,

$$W_1(w) = 0, \tag{58}$$

$$W_2(w) = \frac{2M_A}{M_B}|f_+(w)|^2, \tag{59}$$

$$W_3(w) = 0. \tag{60}$$

(b) For the $0^- \to 1^-$ transition,

$$W_1(w) = \frac{2M_A}{M_B}\left(1 + \frac{M_A}{M_B}\right)^2 A_1^2(w) + \frac{2M_A}{M_B}\frac{4M_A^2}{(M_A+M_B)^2}V^2(w)(w^2-1), \tag{61}$$

$$W_2(w) = \frac{M_B}{2M_A}\left(1 + \frac{M_A}{M_B}\right)^2 A_1^2(w) - \frac{2M_A M_B}{M_A+M_B}V^2(w)\left(1 + \rho - \frac{2M_A}{M_B}w\right) + 2A_1(w)A_2(w)\left(\frac{M_A}{M_B} - w\right) + \frac{2M_A M_B}{(M_A+M_B)^2}A_2^2(w)(w^2-1), \tag{62}$$

$$W_3(w) = \frac{4M_A}{M_B}A_1(w)V(w). \tag{63}$$

The kinematically allowed region is presented in Fig. 3 where the lower bound curve $w_m(x)$ has the shape

$$w_m(x) = \frac{M_B}{2M_A}(1-2x) + \frac{M_A}{2M_B}\frac{1}{1-2x}. \tag{64}$$

The analytical expression for the $d\Gamma/dx$ distribution depends on the q^2 behavior of the form factors. Using (51)–(55), we obtain, after the integration over w,

$$\frac{d\Gamma}{dx} = \frac{G_F^2|V_{ab}|^2 M_B^5}{32\pi^3}\left[e^{-\alpha\frac{w_m(x)-1}{w_m(x)+1}}K_1(x) + \sinh[\alpha\chi_-(x)]e^{-\alpha\chi_+(x)}K_2(x) + K_3(x)\int_{w_m(x)}^{w_0} dw\, e^{-\alpha\frac{w-1}{w+1}}\right], \tag{65}$$

where

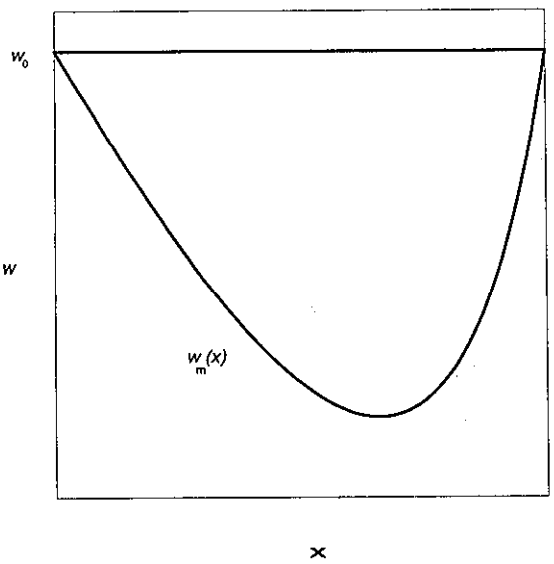

FIG. 3. Allowed region for semileptonic $B \to A(A^*)l\nu_l$ decay in terms of the variables w and x. Lower bound curve $w_m(x)$ is determined by (64), upper bound is $w_0 = (M_A^2 + M_B^2)/(2M_AM_B)$.

$$\chi_-(x) = \frac{4M_AM_B^3}{(M_A+M_B)^4} \frac{x(1-R)}{1-\frac{2M_B^2}{(M_A+M_B)^2}x(1-R)}, \tag{66}$$

$$\chi_+(x) = \left(\frac{M_B-M_A}{M_B+M_A}\right)^2 \frac{1-\frac{M_A^2+M_B^2}{M_B^2-M_A^2}\frac{2M_B^2}{M_B^2-M_A^2}x(1-R)}{1-\frac{2M_B^2}{M_B^2-M_A^2}x(1-R)}, \tag{67}$$

$$R = \frac{\rho}{1-2x}, \quad \rho = \frac{M_A^2}{M_B^2}, \quad \alpha = \frac{4\bar{\Lambda}^2}{\beta_{M_A}^2+\beta_{M_B}^2},$$

$$w_0 = \frac{M_B^2+M_A^2}{2M_AM_B}.$$

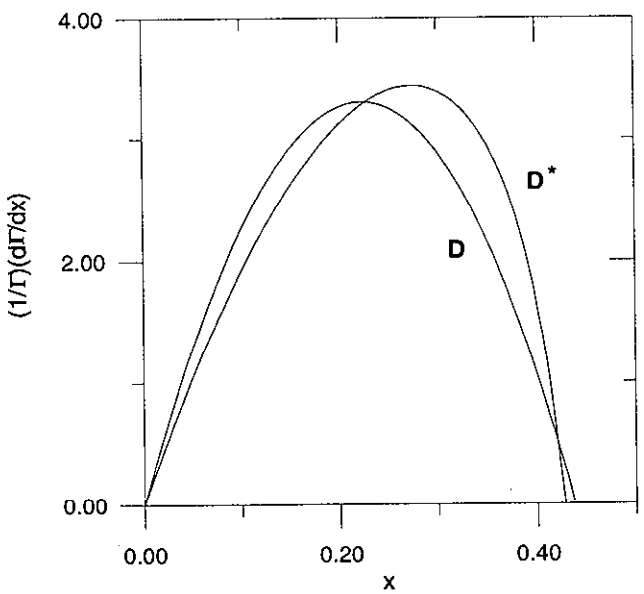

FIG. 4. $(1/\Gamma)(d\Gamma/dx)$ for $B \to Dl\nu_l$ and $B \to D^*l\nu_l$. Absolute rates $d\Gamma/dx$ can be obtained by using $\Gamma(D) = 1.71\times 10^{10}\ s^{-1}$ and $\Gamma(D^*) = 2.92\times 10^{10}\ s^{-1}$ for $\tau_{B^0} = 1.5\times 10^{-12}$ s and $|V_{bc}| = 0.036$.

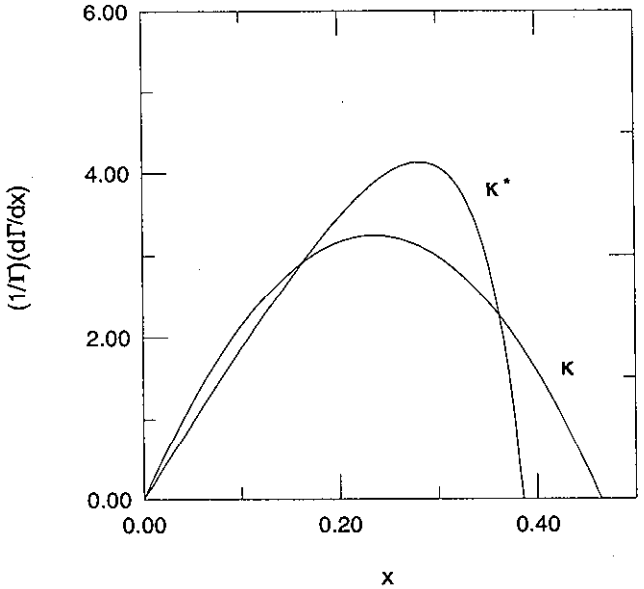

FIG. 5. $(1/\Gamma)(d\Gamma/dx)$ for $D \to Kl\nu_l$ and $D \to K^*l\nu_l$. Absolute rates $d\Gamma/dx$ can be obtained by using $\Gamma(K) = 6.68\times 10^{10}\ s^{-1}$ and $\Gamma(K^*) = 4.34\times 10^{10}\ s^{-1}$ for $\tau_{D^0} = 0.415\times 10^{-12}$ s and $\tau_{D^+} = 1.06\times 10^{-12}$ s.

The functions $K_{1,2,3}(x)$ take different forms for the $0^- \to 0^-$ and $0^- \to 1^-$ decays and are given in Appendix B.

The $(1/\Gamma)(d\Gamma/dx)$ distributions for the $B \to D(D^*)l\nu_l$, $D \to K(K^*)l\nu_l$, and $D_s \to \varphi l\nu_l$ decays are shown in Figs. 4–6. All curves are normalized by the corresponding decay width Γ, i.e., the area under each curve is equal to 1.

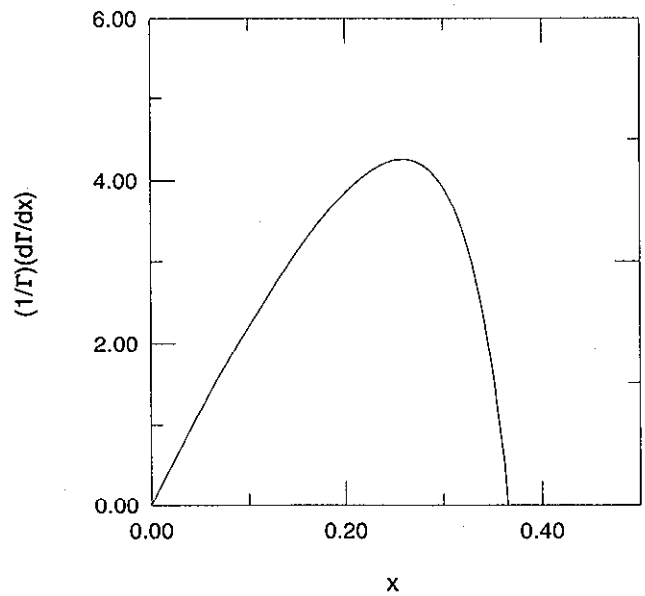

FIG. 6. $(1/\Gamma)(d\Gamma/dx)$ for $D_s \to \phi l\nu_l$. Absolute rate $d\Gamma/dx$ can be obtained by using $\Gamma = 5.42\times 10^{10}\ s^{-1}$ for $\tau_{D_s} = 0.47\times 10^{-12}$ s.

IV. CONCLUSION

Using the quasipotential approach, we have obtained expressions for the semileptonic decay form factors taking consistent account of relativistic effects. This account includes more careful consideration of the s quark contribution than in our previous work [15] and results in a small shift in the values of the $D \to K(K^*)l\nu_l$ decay form factors, which are in good agreement with measurements. Our model provides more accurate values for the ratio $A_2(0)/A_1(0)$ in the $D \to K(K^*)l\nu_l$ decay and for the ratio $\Gamma(D \to K^*l\nu_l)/\Gamma(D \to Kl\nu_l)$ in comparison with other models. We have also calculated form factors and branching ratios for $B \to D(D^*)l\nu_l$, $D \to K(K^*)l\nu_l$, and $D_s \to \varphi l\nu_l$. The extracted value of $|V_{cb}| = 0.036 \pm 0.001 \pm 0.004$ is lower than the previous one [15] because of the changes in the form factors as well as in the B meson lifetime. We should emphasize that in order to get reliable results for D meson semileptonic decays it is necessary to take into consideration all possible relativistic effects, including the transformation of the meson wave function (20) from the rest frame, which is ignored in many quark models.

The proposed q^2 dependence of the form factors is used for the determination of differential semileptonic distributions in the case of pseudoscalar and vector final states.

It should be noted that the expressions obtained for the semileptonic form factors are valid for all B and D meson decays, except decays into mesons containing two light quarks (π, ρ mesons), where one cannot expand in either $\mathbf{p}^2/m^2$ or $\mathbf{p}^2/\varepsilon^2$ at the $q^2 = q^2_{\max}$ point in the vertex function (19). The solution of this problem is proposed in [35].

The analysis has shown that the Lorentz structure of the quark-antiquark potential plays an important role in heavy meson semileptonic decays. We have obtained experimentally motivated and HQET-based arguments to conclude that the confining potential has predominantly a Lorentz vector (with Pauli term) structure $\varepsilon = -1$. Assuming also the long-range anomalous chromomagnetic moment of the quark to be $\kappa = -1$ we have obtained satisfactory description of all considered B and D semileptonic decays.

We argue that the small number of parameters, most of which were fixed previously, and the agreement with HQET for the structure of leading, subleading, and second order terms in the $1/m_Q$ expansion make the RQM a reliable tool for the investigation of heavy meson physics.

In this paper we have restricted ourselves to the $0^- \to 0^-$ and $0^- \to 1^-$ transitions. One more practically important case of decay into a P wave final state (i.e., $B \to D^{**}l\nu_l$) will be considered in the future.

ACKNOWLEDGMENTS

We would like to thank B.A. Arbuzov, M. Beyer, A.G. Grozin, J.G. Körner, T. Mannel, V.A. Matveev, M. Neubert, V.I. Savrin, and A.I. Studenikin for their interest in our work and helpful discussions. We also wish to thank the Interregional Centre for Advanced Studies (Moscow) for kind hospitality during all stages of this work. This research was supported in part by the Russian Foundation for Fundamental Research under Grant No. 94-02-03300-a.

APPENDIX A: EXCLUSIVE SEMILEPTONIC DECAY FORM FACTORS AT $q^2 = q^2_{\max}$ POINT

$$f_+^{(1)}(q^2_{\max}) = \sqrt{\frac{M_A}{M_B}} \int \frac{d^3\mathbf{p}}{(2\pi)^3} \bar{\Psi}_A(\mathbf{p}) \left(\frac{\varepsilon_a + m_a}{2\varepsilon_a}\right)^{1/2} \left\{1 + \frac{M_B - M_A}{\varepsilon_a + m_a} - \frac{\mathbf{p}^2}{8}\left[\frac{1}{m_b^2} - \frac{4}{m_b(\varepsilon_a + m_a)}\right.\right.$$
$$+ \frac{M_B - M_A}{\varepsilon_a + m_a}\left(\frac{1}{m_b^2} + \frac{4}{\varepsilon_a(\varepsilon_a + m_a)} + \frac{2}{3\varepsilon_a m_a}\right) + \frac{4}{3}\frac{M_B - M_A}{M_A}\left(\frac{1}{\varepsilon_a + m_a} - \frac{1}{2m_b}\right)\left.\frac{\varepsilon_a - \varepsilon_q}{\varepsilon_a \varepsilon_q}\right]$$
$$\left. + \frac{M_B - M_A}{3}\left[\frac{1}{\varepsilon_a + m_a} + \frac{1}{2m_b} - \frac{\mathbf{p}^2}{8m_b^2}\left(\frac{1}{\varepsilon_a + m_a} + \frac{3}{2m_b}\right)\right]\frac{\varepsilon_q}{M_A}\left(\mathbf{p}\frac{\overleftarrow{\partial}}{\partial \mathbf{p}}\right)\right\}\Psi_B(\mathbf{p}), \tag{A1}$$

$$f_{+S}^{(2)}(q^2_{\max}) = \sqrt{\frac{M_A}{M_B}} \int \frac{d^3\mathbf{p}}{(2\pi)^3} \bar{\Psi}_A(\mathbf{p}) \left(\frac{\varepsilon_a + m_a}{2\varepsilon_a}\right)^{1/2} \left[-\frac{M_B - M_A}{2\varepsilon_a}\frac{M_B - \varepsilon_b - \varepsilon_q}{\varepsilon_a} + \frac{M_B - M_A}{12\varepsilon_a}\mathbf{p}^2\right.$$
$$\left. \times \left(\frac{1}{\varepsilon_a^2} + \frac{1}{m_b^2}\right) - \frac{M_B - M_A}{12}\left(\frac{1}{\varepsilon_a^2} + \frac{1}{m_b^2}\right)(M_B + M_A - \varepsilon_b - \varepsilon_a - 2\varepsilon_q)\frac{\varepsilon_q}{M_A}\left(\mathbf{p}\frac{\overleftarrow{\partial}}{\partial \mathbf{p}}\right)\right]\Psi_B(\mathbf{p}), \tag{A2}$$

$$f_{+V}^{(2)}(q^2_{\max}) = \sqrt{\frac{M_A}{M_B}} \int \frac{d^3\mathbf{p}}{(2\pi)^3} \bar{\Psi}_A(\mathbf{p}) \left(\frac{\varepsilon_a + m_a}{2\varepsilon_a}\right)^{1/2} \left\{\frac{M_B - M_A}{\varepsilon_a}\frac{\mathbf{p}^2}{12}\left[(1+\kappa)\left(\frac{1}{\varepsilon_a^2} - \frac{1}{m_b^2}\right) - \frac{1}{\varepsilon_q}\left(\frac{2}{\varepsilon_a + m_a} + \frac{1}{m_b}\right)\right]\right.$$
$$+ \frac{M_B - M_A}{12}(1+\kappa)\left(\frac{1}{\varepsilon_a^2} - \frac{1}{m_b^2}\right)(M_B - M_A - \varepsilon_q + \varepsilon_a)\frac{\varepsilon_q}{M_A}\left(\mathbf{p}\frac{\overleftarrow{\partial}}{\partial \mathbf{p}}\right)$$
$$\left. + \frac{M_B - M_A}{6\varepsilon_q}\left(\frac{1}{\varepsilon_a + m_a} + \frac{1}{2m_b}\right)(M_B + M_A - \varepsilon_b - \varepsilon_a - 2\varepsilon_q)\frac{\varepsilon_q}{M_A}\left(\mathbf{p}\frac{\overleftarrow{\partial}}{\partial \mathbf{p}}\right)\right\}\Psi_B(\mathbf{p}), \tag{A3}$$

$$A_1^{(1)}(q^2_{\max}) = (M_A+M_B)\sqrt{4M_AM_B}\int\frac{d^3\mathbf{p}}{(2\pi)^3}\bar{\Psi}_A(\mathbf{p})\left(\frac{\varepsilon_a+m_a}{2\varepsilon_a}\right)^{1/2}\left[1-\frac{\mathbf{p}^2}{8}\left(\frac{1}{m_b^2}+\frac{4}{3(\varepsilon_a+m_a)m_b}\right)\right]\Psi_B(\mathbf{p}), \tag{A4}$$

$$A_{1S}^{(2)}(q^2_{\max}) = A_{1V}^{(2)}(q^2_{\max}) = 0, \tag{A5}$$

$$\begin{aligned}A_2^{(1)}(q^2_{\max}) = {}& \frac{1}{(M_A+M_B)\sqrt{4M_AM_B}}\int\frac{d^3\mathbf{p}}{(2\pi)^3}\bar{\Psi}_A(\mathbf{p})\left(\frac{\varepsilon_a+m_a}{2\varepsilon_a}\right)^{1/2}\\ &\times\left(\left(1+\frac{M_A}{M_B}\right)\left[1-\frac{\mathbf{p}^2}{2}\left(\frac{1}{4m_b^2}+\frac{1}{3m_b(\varepsilon_a+m_a)}\right)\right]-\frac{2M_A^2}{M_B(\varepsilon_a+m_a)}\right.\\ &\times\left[1-\frac{\mathbf{p}^2}{8}\left(\frac{1}{m_b^2}+\frac{4}{\varepsilon_a(\varepsilon_a+m_a)}+\frac{2}{3\varepsilon_am_b}\right)-\frac{\mathbf{p}^2}{6M_A\varepsilon_a}\left(1+\frac{\varepsilon_a+m_a}{2m_b}\right)\right]\\ &-\frac{2M_A\varepsilon_q}{(\varepsilon_a+m_a)M_B}\left\{\frac{1}{3}\left[1+\frac{\varepsilon_a+m_a}{2m_b}-\frac{\mathbf{p}^2}{8m_b^2}\left(1+\frac{3(\varepsilon_a+m_a)}{2m_b}\right)\right]\right.\\ &\left.\left.+\frac{M_B-M_A}{3m_b}\left(1-\frac{3\mathbf{p}^2}{8m_b^2}\right)\right\}\left(\mathbf{p}\frac{\overleftarrow{\partial}}{\partial\mathbf{p}}\right)\right)\Psi_B(\mathbf{p}),\end{aligned} \tag{A6}$$

$$\begin{aligned}A_{2S}^{(2)}(q^2_{\max}) = {}& \frac{1}{(M_A+M_B)\sqrt{4M_AM_B}}\int\frac{d^3\mathbf{p}}{(2\pi)^3}\bar{\Psi}_A(\mathbf{p})\left(\frac{\varepsilon_a+m_a}{2\varepsilon_a}\right)^{1/2}\frac{M_A^2}{\varepsilon_aM_B}\left[-\frac{M_B-\varepsilon_b-\varepsilon_q}{\varepsilon_a}\right.\\ &\left.+\frac{\mathbf{p}^2}{6}\left(\frac{1}{\varepsilon_a^2}+\frac{1}{m_b^2}\right)-\frac{\varepsilon_a}{6}(M_B+M_A-\varepsilon_b-\varepsilon_a-2\varepsilon_q)\left(\frac{1}{\varepsilon_a^2}+\frac{1}{m_b^2}\right)\frac{\varepsilon_q}{M_A}\left(\mathbf{p}\frac{\overleftarrow{\partial}}{\partial\mathbf{p}}\right)\right]\Psi_B(\mathbf{p}),\end{aligned} \tag{A7}$$

$$\begin{aligned}A_{2V}^{(2)}(q^2_{\max}) = {}& \frac{1}{(M_A+M_B)\sqrt{4M_AM_B}}\int\frac{d^3\mathbf{p}}{(2\pi)^3}\bar{\Psi}_A(\mathbf{p})\left(\frac{\varepsilon_a+m_a}{2\varepsilon_a}\right)^{1/2}\left\{\frac{M_A^2}{\varepsilon_aM_B}\left[\frac{\mathbf{p}^2}{6}(1+\kappa)\right.\right.\\ &\left.\times\left(\frac{1}{\varepsilon_a^2}-\frac{1}{m_b^2}\right)+\frac{\varepsilon_a}{6}(M_B-M_A-\varepsilon_b+\varepsilon_a)(1+\kappa)\left(\frac{1}{\varepsilon_a^2}-\frac{1}{m_b^2}\right)\frac{\varepsilon_q}{M_A}\left(\mathbf{p}\frac{\overleftarrow{\partial}}{\partial\mathbf{p}}\right)\right]\\ &\left.-\frac{\mathbf{p}^2}{6\varepsilon_q}\left(\frac{2}{\varepsilon_a+m_a}+\frac{1}{m_b}\right)+\frac{\varepsilon_a}{6M_A}\left(\frac{2}{\varepsilon_a+m_a}+\frac{1}{m_b}\right)(M_B+M_A-\varepsilon_b-\varepsilon_a-2\varepsilon_q)\left(\mathbf{p}\frac{\overleftarrow{\partial}}{\partial\mathbf{p}}\right)\right\}\Psi_B(\mathbf{p}),\end{aligned} \tag{A8}$$

$$\begin{aligned}V^{(1)}(q^2_{\max}) = {}& \frac{1}{M_A+M_B}\sqrt{\frac{M_A}{M_B}}\int\frac{d^3\mathbf{p}}{(2\pi)^3}\bar{\Psi}_A(\mathbf{p})\left(\frac{\varepsilon_a+m_a}{2\varepsilon_a}\right)^{1/2}\frac{1}{\varepsilon_a+m_a}\left\{1-\frac{\mathbf{p}^2}{8}\left(\frac{1}{m_b^2}\right.\right.\\ &\left.+\frac{4}{\varepsilon_a(m_a+\varepsilon_a)}-\frac{2}{3\varepsilon_am_b}\right)-\frac{\mathbf{p}^2}{12M_A}\left(1+\frac{\varepsilon_a+m_a}{2m_b}\right)\frac{\varepsilon_a+\varepsilon_q}{\varepsilon_a\varepsilon_q}-\frac{\mathbf{p}^2}{12M_A\varepsilon_a}\left(1-\frac{\varepsilon_a+m_a}{2m_b}\right)\\ &\left.+\frac{1}{3}\left[1-\frac{\varepsilon_a+m_a}{2m_b}-\frac{\mathbf{p}^2}{8m_b^2}\left(1+\frac{3(\varepsilon_a+m_a)}{2m_b}\right)\right]\frac{\varepsilon_q}{M_A}\left(\mathbf{p}\frac{\overleftarrow{\partial}}{\partial\mathbf{p}}\right)\right\}\Psi_B(\mathbf{p}),\end{aligned} \tag{A9}$$

$$\begin{aligned}V_S^{(2)}(q^2_{\max}) = {}& \frac{1}{M_A+M_B}\sqrt{\frac{M_A}{M_B}}\int\frac{d^3\mathbf{p}}{(2\pi)^3}\bar{\Psi}_A(\mathbf{p})\left(\frac{\varepsilon_a+m_a}{2\varepsilon_a}\right)^{1/2}\frac{1}{2\varepsilon_a}\left[-\frac{M_B-\varepsilon_b-\varepsilon_q}{\varepsilon_a}\right.\\ &\left.+\frac{\mathbf{p}^2}{6}\left(\frac{1}{\varepsilon_a^2}-\frac{1}{m_b^2}\right)-\frac{\varepsilon_a}{6}(M_B+M_A-\varepsilon_b-\varepsilon_a-2\varepsilon_q)\left(\frac{1}{\varepsilon_a^2}-\frac{1}{m_b^2}\right)\frac{\varepsilon_q}{M_A}\left(\mathbf{p}\frac{\overleftarrow{\partial}}{\partial\mathbf{p}}\right)\right]\Psi_B(\mathbf{p}),\end{aligned} \tag{A10}$$

$$V_V^{(2)}(q^2_{\max}) = \frac{1}{M_A+M_B}\sqrt{\frac{M_A}{M_B}}\int\frac{d^3\mathbf{p}}{(2\pi)^3}\bar{\Psi}_A(\mathbf{p})\left(\frac{\varepsilon_a+m_a}{2\varepsilon_a}\right)^{1/2}\frac{1}{2\varepsilon_a}\left\{\left[\frac{\mathbf{p}^2}{6}+\frac{\varepsilon_a}{6}\right.\right.$$
$$\times(M_B-M_A-\varepsilon_b+\varepsilon_a)\frac{\varepsilon_q}{M_A}\left(\mathbf{p}\frac{\overleftarrow{\partial}}{\partial\mathbf{p}}\right)\Big](1+\kappa)\Big[\frac{1}{\varepsilon_a^2}+\frac{1}{m_b^2}-\frac{1}{\varepsilon_q}\Big(\frac{2}{\varepsilon_a+m_a}+\frac{1}{m_b}\Big)\Big]$$
$$-\frac{\mathbf{p}^2\varepsilon_a}{6\varepsilon_q}\Big(\frac{2}{\varepsilon_a+m_a}-\frac{1}{m_b}\Big)+\frac{\varepsilon_a}{6M_A}(M_B+M_A-\varepsilon_b-\varepsilon_a-2\varepsilon_q)$$
$$\left.\times\Big(\frac{2}{\varepsilon_a+m_a}-\frac{1}{m_b}\Big)\left(\mathbf{p}\frac{\overleftarrow{\partial}}{\partial\mathbf{p}}\right)\right\}\Psi_B(\mathbf{p}); \tag{A11}$$

here $(\mathbf{p}\overleftarrow{\partial/\partial\mathbf{p}})$ acts to the left on the wave function $\bar{\Psi}_A(\mathbf{p})$. In the limit $\mathbf{p}^2/m^2\to 0$ the above form factors reduce to the standard expressions, obtained in the nonrelativistic quark models.

APPENDIX B: FUNCTIONS $K_{1,2,3}(x)$ FOR $(1/\Gamma)d\Gamma/dx$ DIFFERENTIAL DISTRIBUTIONS

(a) In the case of the $0^-\to 0^-$ transition,

$$K_1(x) = \frac{2M_A}{M_B}x(1-2x)(1-R)|f_+(1)|^2, \tag{B1}$$
$$K_2(x) = \frac{2M_A}{M_B}\left(1+\frac{M_A}{M_B}\right)^2(1-2x)|f_+(1)|^2, \tag{B2}$$
$$K_3(x) = \frac{M_A}{M_B}\left(\rho+(1-2x)^2+\frac{2M_A}{M_B}(1-2x)-\frac{4M_A}{M_B}\alpha(1-2x)\right)|f_+(1)|^2. \tag{B3}$$

(b) In the case of the $0^-\to 1^-$ transition,

$$K_1(x) = \frac{M_B}{M_A}x(1-R)\left(G_1(x)+\alpha G_2(x)+\frac{2}{3}\alpha^2G_3(x)\right)+\frac{1}{2}\left(G_2(x)+\frac{2}{3}\alpha G_3(x)\right)$$
$$\times\left[x(1-r)\left(1+\frac{M_B}{M_A}\right)^2-\frac{M_B^2}{M_A^2}x^2(1-R)^2\right]+\frac{1}{3}G_3(x)\Big(\frac{3M_B}{M_A}x(1-R)\frac{(M_A+M_B)^4}{4M_A^2M_B^2}$$
$$+\frac{3M_B^2}{M_A^2}\frac{(M_A+M_B)^2}{2M_AM_B}x^2(1-R)^2-\frac{(M_A+M_B)^6}{8M_A^3M_B^3}x^3(1-R)^3\Big), \tag{B4}$$

$$K_2(x) = -\frac{(M_A+M_B)^2}{M_AM_B}\left(G_1(x)+\alpha G_2(x)+\frac{2}{3}\alpha^2G_3(x)\right)$$
$$-\frac{(M_A+M_B)^4}{M_A^2M_B^2}\left(G_2(x)+\frac{2}{3}\alpha G_3(x)\right)-\frac{(M_A+M_B)^6}{12M_A^3M_B^3}G_3(x), \tag{B5}$$

$$K_3(x) = -G_4(x)-2\alpha G_1(x)-2\alpha^2G_2(x)-\frac{4}{3}\alpha^3G_3(x), \tag{B6}$$

where $G_{1,2,3,4}(x)$ depend on the values of the form factors at the $w=1$ point:

$$G_1(x) = V^2(1)\left[\frac{16M_A^2}{(M_A+M_B)^2}\Big(1-2x+\frac{M_A}{M_B}\Big)^2-\frac{16M_A^2}{M_B^2}\Big(1-2x+\frac{2M_A}{M_B}\Big)\right]$$
$$+\frac{16M_AM_B}{(M_A+M_B)^2}A_2^2(1)\Big(1-2x+\frac{M_A}{M_B}\Big)^2-\frac{8M_A}{M_B}A_1(1)V(1)\Big(1+\frac{M_A}{M_B}\Big)^2\Big(1-2x+\frac{M_A}{M_B}\Big)$$
$$-\frac{4M_A}{M_B}A_1(1)A_2(1)\Big(1+\frac{M_B}{M_A}\Big)\Big(1-2x+\frac{M_A}{M_B}\Big)^2, \tag{B7}$$

$$G_2(x)=\frac{16M_A^2}{(M_A+M_B)^2}\frac{M_A}{M_B}V^2(1)\left[2(1-2x)+\left(1+\frac{M_A}{M_B}\right)^2+\frac{4M_A}{M_B}\right]-\frac{8M_AM_B}{(M_A+M_B)^2}A_2^2(1)$$
$$\times\left[\left(1-2x+\frac{M_A}{M_B}\right)^2+\frac{4M_A}{M_B}(1-2x)\right]+\frac{M_A}{M_B}A_1^2(1)\left(1+\frac{M_A}{M_B}\right)^2\left[\left(1+\frac{M_A}{M_B}\right)^2\right.$$
$$\left.\times\frac{M_B^2}{2M_A^2}\left(1-2x+\frac{M_A}{M_B}\right)^2\right]+\frac{8M_A^2}{M_B^2}A_1(1)V(1)\left[2(1-2x)+\left(1+\frac{M_A}{M_B}\right)^2+\frac{2M_A}{M_B}\right]$$
$$+4A_1(1)A_2(1)\left(1-2x+\frac{M_A}{M_B}\right)^2+\frac{8M_A}{M_B}A_2(1)A_1(1)(1-2x)\left(1+\frac{M_A}{M_B}\right), \tag{B8}$$

$$G_3(x)=-\frac{8M_A}{M_B}A_1(1)A_2(1)(1-2x)-\frac{16M_A^3}{M_B^3}A_1(1)V(1)+\frac{16M_A^2}{(M_A+M_B)^2}\left(A_2^2(1)(1-2x)\right.$$
$$\left.-\frac{2M_A^2}{M_B^2}V^2(1)\right)+\frac{2M_A^2}{M_B^2}\left(1+\frac{M_A}{M_B}\right)^2A_1^2(1)\left(-1+\frac{M_B^2}{2M_A^2}(1-2x)\right), \tag{B9}$$

$$G_4(x)=\frac{8M_AM_B}{(M_A+M_B)^2}V^2(1)\left(1+\frac{M_A}{M_B}\right)^2\left(1-2x+\frac{M_A}{M_B}\right)^2. \tag{B10}$$

[1] N. Isgur, D. Scora, B. Grinstein, and M.B. Wise, Phys. Rev. D **39**, 799 (1989).
[2] M. Wirbel, B. Stech, and M. Bauer, Z. Phys.C **29**, 627 (1985); **42**, 671 (1989).
[3] T. Altomari and L. Wolfenstein, Phys. Rev. D **37**, 681 (1988).
[4] C. Bernard, A. El Khadra, and A. Soni, Phys. Rev. D **43**, 2140 (1992).
[5] V. Lubicz, G. Martinelli, M.S. McArthy, and C.T. Sachrajda, Phys. Lett. B **274**, 415 (1992).
[6] P. Ball, V.M. Braun, and H.G. Dosch, Phys. Rev. D **44**, 3567 (1991).
[7] M. Neubert, Phys. Rep. **245**, 259 (1994).
[8] J.F. Amundson and J.L. Rosner, Phys. Rev. D **47**, 1951 (1993).
[9] R.N. Faustov and V.O. Galkin, Z. Phys. C **66**, 119 (1995).
[10] V.O. Galkin, A.Yu. Mishurov, and R.N. Faustov, Yad. Fiz. **55**, 2175 (1992) [Sov. J. Nucl. Phys. **55**, 1207 (1992)].
[11] V.O. Galkin, A.Yu. Mishurov, and R.N. Faustov, Yad. Fiz. **51**, 1101 (1990) [Sov. J. Nucl. Phys. **51**, 705 (1990)].
[12] V.O. Galkin, A.Yu. Mishurov, and R.N. Faustov, Yad. Fiz. **53**, 1676 (1991) [Sov. J. Nucl. Phys. **53**, 1026 (1991)].
[13] R.N. Faustov and V.O. Galkin, Phys. Rev. D **52**, 5131 (1995).
[14] R.N. Faustov, V.O. Galkin, and A.Yu. Mishurov, in *Quarks '92*, Proceedings of the Seventh International Seminar, Zrenigorod, Russia, edited by D. Grigorev *et al.* (World Scientific, Singapore, 1993), p. 326.
[15] V.O. Galkin, A.Yu. Mishurov, and R.N. Faustov, Yad. Fiz. **55**, 1080 (1992) [Sov. J. Nucl. Phys. **55**, 608 (1992)].
[16] A.A. Logunov and A.N. Tavkhelidze, Nuovo Cimento **29**, 380 (1963).
[17] A.P. Martynenko and R.N. Faustov, Teor. Mat. Fiz. **64**, 179 (1985).
[18] D. Gromes, Nucl. Phys. **B131**, 80 (1977).
[19] H. Schnitzer, Phys. Rev. D **18**, 3482 (1978).
[20] R.N. Faustov, Ann. Phys. (N.Y.) **78**, 176 (1973); Nuovo Cimento **69**, 37 (1970).
[21] V.O. Galkin and R.N. Faustov, Teor. Mat. Fiz. **85**, 155 (1990).
[22] F. Gilman and R.J. Singleton, Phys. Rev. D **41**, 142 (1990).
[23] Particle Data Group, L. Montanet *et al.*, Phys. Rev. D **50**, 1173 (1994).
[24] CLEO Collaboration, S. Sanghera *et al.*, Phys. Rev. D **47**, 791 (1993).
[25] N. Isgur and M.B. Wise, Phys. Lett. B **237**, 527 (1990).
[26] M. Neubert *et al.*, in *Heavy Flavors*, edited by A.J. Buras and M. Lindner (World Scientific, Singapore, 1992), p. 286.
[27] ARGUS Collaboration, H. Albrecht *et al.*, Phys. Lett. B **229**, 175 (1989).
[28] CLEO Collaboration, R. Fulton *et al.*, Phys. Rev. D **43**, 651 (1991).
[29] ARGUS Collaboration, H. Albrecht *et al.*, Z. Phys. C **57**, 533 (1993).
[30] CLEO Collaboration, D. Bortoletto *et al.*, Phys. Rev. Lett. **63**, 1667 (1989).
[31] E691 Collaboration, J.C. Anjos *et al.*, Phys. Rev. Lett. **65**, 2630 (1990).
[32] E653 Collaboration, K. Kodama *et al.*, Phys. Lett. B **286**, 187 (1992).
[33] E687 Collaboration, P.L. Frabetti *et al.*, Phys. Lett. B **307**, 262 (1993).
[34] CLEO Collaboration, A. Bean *et al.*, Phys. Lett. B **317**, 647 (1993).
[35] V.O. Galkin, A.Yu. Mishurov, and R.N. Faustov, Phys. Lett. B **356**, 516 (1995).
[36] CLEO Collaboration, P. Avery *et al.*, Phys. Lett. B **337**, 405 (1994).
[37] D. B. Gibaut and D. M. Potter, Mod. Phys. Lett. A **9**, 675 (1994).
[38] Z. Ligetti, Y. Nir, and M. Neubert, Phys. Rev. D **49**, 1302 (1994).